Perturbed-angular-correlation experiments with ^{111}In in MBa$_2$Cu$_3$O$_{7-\delta}$ (M = Y,Yb): The Cu(1)-site puzzle

Axel Bartos and Michael Uhrmacher
II. Physikalisches Institut Universität Göttingen, Bunsenstrasse 7-9, 37073 Göttingen, Germany
(Received 29 April 1993)

Perturbed-angular-correlation spectroscopy has been used to study the hyperfine interaction of ^{111}In implanted into YbBa$_2$Cu$_3$O$_{7-\delta}$. Five different electric field gradients have been observed that depend on the annealing temperature in a similar way as the ones found with the same probe in YBa$_2$Cu$_3$O$_{7-\delta}$. The comparison with the electric field gradients measured at ^{111}Cd in the constituents Yb$_2$Cu$_2$O$_5$ and Y$_2$Cu$_2$O$_5$ clearly demonstrates that the hyperfine interactions previously attributed to the Cu(1) site in YBa$_2$Cu$_3$O$_{7-\delta}$ have their origin in the Y$_2$Cu$_2$O$_5$ structure. A simple model is proposed that embeds a Y$_2$Cu$_2$O$_5$ or a Yb$_2$Cu$_2$O$_5$ microscopic structure between the $(CuO_2)_\infty$ planes of the high-T_c superconductors YBa$_2$Cu$_3$O$_{7-\delta}$ or YbBa$_2$Cu$_3$O$_{7-\delta}$, respectively.

I. INTRODUCTION

In 1986, Bednorz and Müller found a new class of superconductors (La, Ba)$_2$CuO$_4$.[1] Shortly after that, Wu *et al.* were able to improve the transition temperature T_c by replacing La^{3+} with the smaller Y^{3+} and they obtained the well-known high-T_c superconductor YBa$_2$Cu$_3$O$_{7-\delta}$.[2,3] Its structure is characterized by $(CuO)_\infty$ chains with the Cu(1) sites and $(CuO_2)_\infty$ planes with the Cu(2) sites. Today it is generally accepted that the superconductivity occurs along these $(CuO_2)_\infty$ planes in a complex local interaction between structure, stoichiometry, and the charge state of the different atoms.[4]

Perturbed-angular-correlation (PAC) spectroscopy is a highly sensitive tool for studying solids on an atomic scale: in recent years it has been applied successfully to investigate point defects in metals,[5] compounds,[6,7] and semiconductors.[8,9] Dynamical changes of charge states in semiconductors[10,11] and oxides[12,13] have been discussed; the influence of ionic or covalent chemical bonding was studied,[14–16] and the evolution of solid state reactions was studied as well.[17–19] Many studies on binary[14,15,20–22] and ternary[23–25] oxides provided insight into a great number of phase transitions.[17,19,24,26,27] Recent investigations of isostructural oxides of some C-M_2O_3 (Refs. 21 and 22) and $M_2Cu_2O_5$ (Ref. 23) (M = Sc, In, Y, rare earth elements) demonstrated the high sensitivity of the PAC spectroscopy to small structural changes. In the case of C-M_2O_3 it was even possible to relate changes in the hyperfine interaction parameters to structural changes that had not been resolved with conventional diffraction analysis.[21,28,29] Therefore, PAC spectroscopy promised to be a neat tool to study the YBa$_2$Cu$_3$O$_{7-\delta}$ ceramics.

But, on the other hand, valuable information on the local structure can only be obtained if the site location of the probe is known. This is, of course, straightforward if the probe itself belongs to the structure. Unfortunately, neither is indium a constituent element in YBa$_2$Cu$_3$O$_{7-\delta}$, nor is the crystal structure of YBa$_2$Cu$_3$O$_{7-\delta}$ simple: four regular and nonequivalent cation sites already exist despite many different local configurations due to oxygen defects. As a consequence of the complex structure, a lot of different experimental results for ^{111}In(EC)^{111}Cd in YBa$_2$Cu$_3$O$_{7-\delta}$ have been published so far. Their hyperfine interaction parameters are listed in Table I and a short resume of these electric field gradients will be given in Sec. III.

It can be seen from Table I that electric field gradients with the hyperfine interaction parameters $\nu_Q \approx 150$ MHz and $\eta \approx 1$ dominate the PAC spectra for low annealing temperatures ($T_a \lesssim 1100$ K) as found in several investigations.[30–36] In most cases these electric field gradients have been attributed to ^{111}In substituting the Cu(1) site in YBa$_2$Cu$_3$O$_{7-\delta}$. But, as already mentioned by Bartos and Uhrmacher,[37] their hyperfine interaction parameters are extremely similar to those found in the so-called *blue-phase* Y$_2$Cu$_2$O$_5$ (Ref. 23)—a situation that we call the "Cu(1)-site puzzle."

In order to clarify the origin of these electric field gradients we performed the present PAC experiments on ^{111}In in YbBa$_2$Cu$_3$O$_{7-\delta}$. It is a well-known fact that in this family of high T_c ceramics the Y atom can be substituted by nearly all rare earth elements without changing the structure and the superconducting properties.[38,39] Therefore, the electric field gradient at ^{111}Cd on the Cu(1) site in YBa$_2$Cu$_3$O$_{7-\delta}$ should not be affected by a substitution of Y by Yb: one expects to find nearly *identical electric field gradients* at the Cu(1) site in YBa$_2$Cu$_3$O$_{7-\delta}$ *and* in YbBa$_2$Cu$_3$O$_{7-\delta}$. If, on the other hand, these electric field gradients represent a site in Y$_2$Cu$_2$O$_5$ or in Yb$_2$Cu$_2$O$_5$, then the *corresponding electric field gradients* of the different compounds are expected. The substitution of Y by Yb was just chosen because of the distinct difference between the hyperfine interaction parameters of ^{111}In(EC)^{111}Cd in Y$_2$Cu$_2$O$_5$ and in Yb$_2$Cu$_2$O$_5$.[23]

TABLE I. Review of electric-field gradients found with ^{111}In(EC)^{111}Cd in $YBa_2Cu_3O_{7-\delta}$. The sample–preparation information and the proposed site allocation are taken from the given references. Our abbrevations used in the text are given in column 6.

P[a]	T[b]	at[c]	T_c [K][d]	x[e]	f_Y(i)	ν_Q [MHz]	η	ω_1 [MHz]	Site	Ref.	Remarks[f]
i	925	o	LN	6.9	$f_Y(1)$	143(1)	1	238	Cu(1)	34	X(+),OT(+)
					$f_Y(2)$	156(1)	1	259	Cu(1)		
						156(2)	0	147			
i	985	v		6.0		134(1)	0	126	Cu(1)	34	X(+),OT(+)
d	1015	o			$f_Y(1)$	139.6(8)	1	232		33	
					$f_Y(2)$	155.9(8)	1	259			
i	1075	o	LN		$f_Y(1,2)$	149(3)	0.95(5)	240	Cu(1)	35	
						47(1)	0.8(1)	68			
						133(5)	0.3(1)	137			
						106(5)	0.4(1)	116			
						34(1)	0.4(1)	37	Y		
d	1100	o		6.92	$f_Y(1,2)$	145(2)	1	241	Cu(1)	31, 32	OT(-)
		ar		6.78		57.6(5)	0.25	58			
d	1173	o	91	6.95	$f_Y(4)$	39.4(9)	0.29	40	Y	33	
					$f_Y(5)$	139(1)	0.39	151	Ba		
s	1215				$f_Y(4)$	39(5)	0.34(15)	41	Y	12	O T(+), X(-)
					$f_Y(5)$	133(2)	0.41(6)	146	Cu		
d	1220	o	91		$f_Y(4)$	38.6(1)	0.37(1)	41	Y	62	
c	1220	o	94			90(5)	0.12	86		75	X(+)
						107(5)	0.35	114			
n	1225	a				68(1)	0.5(1)	80		76	X (-)
n	1225		93			54	0.28	55		30	OT(-)
								240			
d	1245	o			$f_Y(4)$	38(1)	0.37(6)	41	Y	61	
						49(8)	0.58(4)	61	Y		
						142(3)	0.34(3)	150			Y_2O_3

[a] Sample preparation: n: nitrate decomposition, c: calcination in air, s: sol gel synthesis, d: ^{111}In evaporation and in diffusion, i: ^{111}In implantation.

[b] Highest preparation temperature.

[c] Sample prepared in oxygen atmosphere: o, air: a, vacuum: v, argon: ar.

[d] LN: superconducting at least at T=77 K.

[e] Oxygen stoichiometry parameter x: ($YBa_2Cu_3O_x$).

[f] Single phase product: X(+), multiple phases: X(-), detected by x–ray analysis. Change: OT(+) or no change: OT(-) of hyperfine interaction parameters during the orthorhombic-to-tetragonal phase transition.

II. EXPERIMENTAL DETAILS

A. PAC spectroscopy

The PAC spectroscopy has previously been reviewed in detail.[8,40–44] In a typical PAC experiment, probe atoms ^{111}In(EC)^{111}Cd are introduced into a matrix and interact with electric-field gradients and/or magnetic hyperfine field(s) produced by the surrounding atoms. The hyperfine interaction is traced via the $\gamma-\gamma$ cascade of the radioactive decay. The first γ transition populates the sensitive $I = 5/2^+$ state, which is characterized by its nuclear moments [$Q = 0.83(13)b$, $\mu_I = 0.572\mu_K$] and the lifetime $\tau = 122$ ns.[40] The hyperfine interaction(s) lead(s) to a precession of the nuclear spin and thus to a time modulation of the probability $W(\Theta,t)$ to find the second γ quant under an angle Θ with respect to the emission direction of the first transition. For ^{111}In(EC)^{111}Cd and in the case of a polycrystalline sample, this probability is given by

$$W(\Theta,t) = 1 + A_{22}\ G_{22}(t)\ P_2(\cos\Theta) \tag{1}$$

where A_{22} denotes the anisotropy coefficient of the $\gamma-\gamma$ cascade and $P_2(\cos\Theta)$ is the second Legendre polynomial. All physical information is included in the time dependent perturbation factor $G_{22}(t)$. It can be extracted from the four $N(\Theta = 180°, t)$ and the eight $N(\Theta = 90°, t)$ coincidence spectra by calculating the perturbation function $R(t)$:

$$R(t) = 2\frac{N(\Theta = 180°, t) - N(\Theta = 90°, t)}{N(\Theta = 180°, t) + 2N(\Theta = 90°, t)} \tag{2}$$

that can be parametrized by the following expression

$$R(t) = A_{22}^{\exp}\sum_{i=1}^{5} f(i)G_{22}^i(t) \tag{3}$$

with $A_{22}^{\exp}$ being the experimental anisotropy coefficient. The perturbation factor $G_{22}^i(t)$ is given by the expression

$$G_{22}^i(t) = \sum_{n=0}^{3} s_{2n}(\eta^i)\cos[g_n(\eta^i)\nu_Q^i t]\exp[-g_n(\eta^i)\delta_Q^i t]\,. \tag{4}$$

The electric field gradient is characterized by the quadrupole coupling constant $\nu_Q^i = eQV_{zz}^i/h$, the asym-

metry parameter $\eta = (V^i_{xx} - V^i_{yy})/V^i_{zz}$ (assuming $|V^i_{xx}| \leq |V^i_{yy}| \leq |V^i_{zz}|$) and a Lorentzian distribution with the width δ^i_Q. The fraction $f(i)$ contains information on the evolution of the system, whereas the other PAC parameters ν^i_Q, η^i, and δ^i_Q characterize the local surrounding of the probe atom. A Fourier transform of the $R(t)$ pattern displays the three precession frequencies $\omega_n = g_n \nu_Q$ with n=1,2,3 and $\omega_3 = \omega_1 + \omega_2$ ($\eta < 1$). We will use the following nomenclature to characterize the measured hyperfine interactions: either $f_{\mathrm{RE}}(i)$ denotes a specific electric field gradient (i) which is characterized by the hyperfine interaction parameters $\nu^{(i)}_Q, \delta^{(i)}_Q$ and $\eta^{(i)}$ and/or it denotes the number of probes which are subject to this electric field gradient *(i)*; the subscript RE indicates the M atom chosen in $M\mathrm{Ba_2Cu_3O_{7-\delta}}$.

The PAC measurements were carried out using a conventional slow–fast setup as described in Ref. 20. Four cylindrical 2 × 2 in.^{2} NaI(Tl) detectors were arranged in 90° geometry and allowed the simultaneous collection of the twelve coincidence spectra. After correction for the true zero time and accidental background, the $R(t)$ functions were calculated according to Eq. (2) and fitted with Eqs. (4) and

$$F(t) = A^{\mathrm{exp}}_{22} \sum_{i=1}^{5} f(i) G^i_{22}(t) d_n(\omega_n, \tau_{\mathrm{NaI(Tl)}}) \qquad (5)$$

using the FORTRAN routine MINUIT.[45] The term $d_n(\omega_n, \tau_{\mathrm{NaI(Tl)}}) = \exp[-(\omega_n \tau_{\mathrm{NaI(Tl)}})^2/16 \ln 2]$ takes into account the damping of the $R(t)$ oscillations due to the finite time resolution $\tau_{\mathrm{NaI(Tl)}} \approx 4(1)$ ns of the NaI(Tl)–detectors.[46]

B. Sample preparation

1. $YBa_2Cu_3O_{7-\delta}$ and $YbBa_2Cu_3O_{7-\delta}$

All $\mathrm{YBa_2Cu_3O_{7-\delta}}$ and $\mathrm{YbBa_2Cu_3O_{7-\delta}}$ samples were produced by H. Thomas, I. Physikalisches Institut, University of Göttingen. Most of them were prepared using the *direct reaction process*:[47] after mixing the constituent materials $\mathrm{Y_2Cu_2O_5}$ and $\mathrm{Y_2BaCuO_5}$ in the correct molar ratio and grinding them thoroughly, the powders were pressed and sintered for more than one week at $T \approx$ 1215 K in air. A minor number of samples was produced either by *citrate synthesis*[48] or by mixing CuO, $\mathrm{Y_2O_3}$, and $\mathrm{BaCO_3}$ in the stoichiometric ratio. In the latter case, the powder was thoroughly ground and sintered for ≈ 12 h at $T \approx$ 1215 K. This procedure was repeated several times. $\mathrm{YbBa_2Cu_3O_{7-\delta}}$ was produced in the same way, using $\mathrm{Yb_2O_3}$, $\mathrm{BaCO_3}$, and CuO as starting materials. It may be mentioned here that no influence of the preparation method on the experimental results was found. Therefore, in the following, the measurements will not be discerned in this respect. All samples were found to be of high quality with a typical transition temperature of T_c = 92 K. X–ray analysis always verified a single phase product.

2. $Y_2Cu_2O_5$ and $Yb_2Cu_2O_5$

The constituent materials CuO and M_2O_3 (M=Y,Yb) were mixed in the stoichiometric ratio and ground thoroughly. Some of the samples were doped with ^{111}In by dropping an aqueous solution of $^{111}\mathrm{In(NO_3)_3}$ on the mixture. The powders were sintered in an oxygen stream for about 36 h at a temperature of ≈ 1275 K.[23] In this way, deep blue–green products were obtained. X–ray analysis always revealed the correct crystal structure.

C. ^{111}In implantation

Unless indicated otherwise, the PAC probes were introduced via ion implantation. Using the Göttingen heavy–ion implanter IONAS,[49] typically 10^{13} $\mathrm{In^+/cm^2}$ were implanted with an energy of E=400 keV into a mean implantation depth of ≈ 100 nm according to TRIM92 calculations.[50] In this depth, the highest ^{111}In concentration is estimated to be less than ≈ 300 ppm.

It has been shown that the physical properties of $\mathrm{YBa_2Cu_3O_{7-\delta}}$ are very sensitive to irradiation.[51] Even the low fluence during the implantation of the heavy ^{111}In ions is supposed to cause radiation damage, with a main disorder in the oxygen sublattice.[52] In fact, the PAC spectra are strongly broadened after ^{111}In implantation.[35] In order to remove the radiation damage in $\mathrm{YbBa_2Cu_3O_{7-\delta}}$ we followed the annealing sequence established in the experiments with $\mathrm{YBa_2Cu_3O_{7-\delta}}$: the samples were annealed for typically $t = 2-6$ h in oxygen atmospheres of p_{O_2} = 800–1000 hPa O_2 at temperatures between 975 K ≤ T_a ≤ 1275 K (see Sec. IV). Afterwards, the oxygen content was restored by annealing the samples for several hours at $T \approx$ 775 K in an oxygen atmosphere of p_{O_2} = 1000 hPa O_2.

III. THE Cu(1)–SITE PUZZLE

A. The electric-field gradients found in $\mathrm{YBa_2Cu_3O_{7-\delta}}$

Before the results of the experiments with $^{111}\mathrm{In(EC)}^{111}\mathrm{Cd}$ in $\mathrm{YbBa_2Cu_3O_{7-\delta}}$ are presented, a short review of the reported electric field gradients at ^{111}Cd in $\mathrm{YBa_2Cu_3O_{7-\delta}}$ will be given. Table I summarizes the results of different investigations: at annealing temperatures below 1100 K, electric-field gradients with parameters of $\nu_Q \approx$150 MHz and an asymmetry parameter close to $\eta \approx 1$ are found in most of the experiments, irrespective of the preparation mode (implantation or diffusion).[30–36] These hyperfine interactions were shown to be in fact a combination of two electric-field gradients[33] that will be referred to as $f_Y(1)$ and $f_Y(2)$ in the following. In the past, $f_Y(1)$ and $f_Y(2)$ were often attributed to $^{111}\mathrm{In(EC)}^{111}\mathrm{Cd}$ residing at the Cu(1) site in $\mathrm{YBa_2Cu_3O_{7-\delta}}$ for the following reasons: (1) Immediately after implantation of $^{112m}\mathrm{In^+}$ into c–axis oriented $\mathrm{YBa_2Cu_3O_{7-\delta}}$ films, a considerable amount of $^{112m}\mathrm{In^+}$ ions is found to occupy a regular lattice site in $\mathrm{YBa_2Cu_3O_{7-\delta}}$.[53] (2) NMR experiments with

^{63,65}Cu yield an asymmetry parameter of $\eta \approx 1$ for the Cu(1) site,[54] in agreement with the experimental PAC value. (3) These two electric field gradients are also found in a $YBa_2Cu_3O_{7-\delta}$– single crystal[34] which should be the cleanest material available. (4) Reviewing several cation substitution studies on $YBa_2Cu_3O_{7-\delta}$, the trivalent In^{3+} can be assumed to substitute the Cu(1) site.[55–57]

On the other hand, several objections to this interpretation exist: During the orthorhombic–to–tetragonal phase transition mainly the oxygen configuration around the Cu(1) site changes drastically. Although a change of hyperfine interaction parameters is found during the orthorhombic–to–tetragonal transition,[34] it did not follow the well known (p_{O_2}, T)-dependence of this phase transition.[58,59] Additionally, the reoxidation reveals these electric field gradients only at high temperatures which is in disagreement with the bulk status of the sample that had become orthorhombic $YBa_2Cu_3O_{7-\delta}$ much earlier.[34]

As we already mentioned earlier,[37,23] these two electric field gradients are extremely similar to those found in the "blue phase" $Y_2Cu_2O_5$ (see also Fig. 2). In this compound the Cu sites are nearly planar coordinated by four oxygen atoms, quite similar to the case of the Cu(1) site in $YBa_2Cu_3O_{7-\delta}$. However, a recent PAC study on ^{111}In in the series of isostructural $M_2Cu_2O_5$ oxides (M=Sc,In,Y,Yb,Lu,Ho,Tb) clearly showed that ^{111}In substitutes the M sites in all these oxides: the probe resides at the center of an irregular oxygen octahedron.[23] Furthermore, PAC measurements on the disintegration of $Y_2Cu_2O_5$ into $CuYO_2$[60,61] yield electric field gradients with hyperfine interaction parameters similar to those observed during the orthorhombic–to–tetragonal phase transition in $YBa_2Cu_3O_{7-\delta}$.[34] We call this complex experimental situation, that is connected with these electric field gradients in $YBa_2Cu_3O_{7-\delta}$ the "Cu(1)–site puzzle."

At temperatures around 1100 K the site assignment is clearer: at an annealing or diffusion temperature $T_a \approx$ 1075 K, at least one well defined hyperfine interaction $f_Y(4)$ is found, having the parameters $\nu_Q \approx 39$ MHz and $\eta \approx 0.3$ (see Table I). Plank and co-workers[33,62,63] and Polewka[64] attributed this hyperfine interaction to ^{111}In residing at the Y site of $YBa_2Cu_3O_{7-\delta}$. Later, this interpretation was also adopted by Gardener *et al.*[12] The substitution of the Y site by $^{111}In^{3+}$ seems most likely since both elements have the same valency and nearly the same size.[53,65]

Heating the $YBa_2Cu_3O_{7-\delta}$ samples to temperatures above $T_a \gtrsim$ 1100 K, a distribution of electric field gradients is found[60,65] having hyperfine interaction parameters between $\nu_Q \approx$ 50–100 MHz and $0.2 \leq \eta \leq 0.5$. We attributed[36,60,65] these electric-field gradients to ^{111}In located in the so called "green phase:" Y_2BaCuO_5 with its three regular cation sites.[66,67] It is a major impurity phase in $YBa_2Cu_3O_{7-\delta}$ and is often found as a decomposition product at such high temperatures.[68,69] Most of these electric-field gradients are also found at ^{111}Cd in the pure Y_2BaCuO_5 phase.[36,61,60,70]

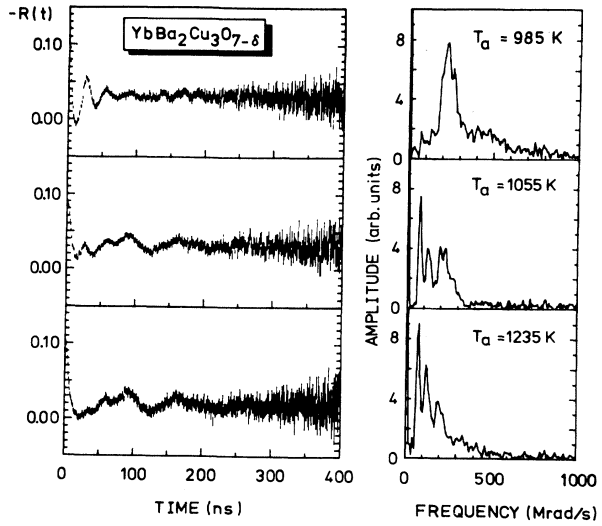

FIG. 1. Perturbation functions $R(t)$ and their corresponding Fourier transforms for ^{111}In(EC)^{111}Cd in $YbBa_2Cu_3O_{7-\delta}$ at the given annealing temperatures.

IV. EXPERIMENTAL RESULTS

A. The electric field gradients found in $YbBa_2Cu_3O_{7-\delta}$

To allow for a comparison with some $YBa_2Cu_3O_{7-\delta}$ experiments already published,[33–35,53] the ^{111}In(EC)^{111}Cd–implanted $YbBa_2Cu_3O_{7-\delta}$ samples were thermally treated in the following sequence: after an annealing at the temperature $T_a = 985$ K, two well defined hyperfine interactions labeled $f_{Yb}(1)$ and $f_{Yb}(2)$ and a broad distribution of electric field gradients $f_{Yb}(3)$ were found. The corresponding $R(t)$ pattern is given in Fig. 1 and is described by the following set of hyperfine interaction parameters:

$$f_{Yb}(1) = 31(2)\ \%,\ \nu_Q = 138(1)\ \text{MHz},\ \delta_Q = 10(1)\ \%,\ \eta = 0.89(1)\ ,$$
$$f_{Yb}(2) = 31(2)\ \%,\ \nu_Q = 154(1)\ \text{MHz},\ \delta_Q = 6(1)\%,\ \eta = 0.83(1)\ ,$$
$$f_{Yb}(3) = 38(4)\ \%,\ \nu_Q = 170(10)\ \text{MHz},\ \delta_Q = 16(5)\ \%,\ \eta = 0.7(2)\ .$$

The analysis of the $R(t)$ spectra always revealed a ratio of the fractions $f_{Yb}(1)/f_{Yb}(2) \approx 1$. Therefore, in the following fits, they were restricted to $f_{Yb}(1) = f_{Yb}(2)$. In a second annealing step, the temperature was raised to $T_a = 1055$ K. This resulted in two new hyperfine interactions, $f_{Yb}(4)$ and $f_{Yb}(5)$ having the hyperfine parameters:

$$f_{Yb}(4) = 50(2)\ \%,\ \nu_Q = 68.5(7)\ \text{MHz},\ \delta_Q = 9(1)\ \%,\ \eta = 0.41(1)\ ,$$
$$f_{Yb}(5) = 40(5)\ \%,\ \nu_Q = 165(3)\ \text{MHz},\ \delta_Q = 20(5)\ \%,\ \eta = 0.45(5)\ .$$

These hyperfine interactions were also found after a further annealing step at the temperature $T_a = 1225$ K.

Now we are able to compare the results obtained for ^{111}In(EC)^{111}Cd in $YBa_2Cu_3O_{7-\delta}$ and in $YbBa_2Cu_3O_{7-\delta}$. First, one notes a similar behavior of the observed hyperfine interaction parameters during the annealing sequence: at high annealing temperatures, i.e., at $T_a \gtrsim 1100$ K, the hyperfine interactions $f_{Yb}(4)$ and $f_{Yb}(5)$ are comparable to $f_Y(4)$ and $f_Y(5)$ found in $YBa_2Cu_3O_{7-\delta}$; they show nearly the same asymmetry parameter $\eta \approx 0.4$ and differ only in the magnitude of their coupling constant by ≈ 30 MHz.

At annealing temperatures below $T_a \lesssim 1000$ K, two well defined hyperfine interactions $f_{RE}(1)$, $f_{RE}(2)$ and a broadly distributed one $f_{RE}(3)$, (RE = Y,Yb) are found in both systems. Figure 2 displays the $R(t)$ perturbation functions with their corresponding Fourier transforms of ^{111}Cd in $MBa_2Cu_3O_{7-\delta}$ and ^{111}Cd in $M_2Cu_2O_5$ (M=Y,Yb). The Fourier spectra reveal clear similarities between $YBa_2Cu_3O_{7-\delta}$ and $Y_2Cu_2O_5$, respectively, between $YbBa_2Cu_3O_{7-\delta}$ and $Yb_2Cu_2O_5$, whereas the spectra measured in the $MBa_2Cu_3O_{7-\delta}$ structures are different. This impression is confirmed if one compares the fitted parameters given in Table II. The spectra had been analyzed with a three site model to allow for a direct comparison of the fits. A clear difference of the hyperfine interaction parameters of ^{111}Cd in $YBa_2Cu_3O_{7-\delta}$ and in $YbBa_2Cu_3O_{7-\delta}$ is found, but they agree well with those found in the corresponding $M_2Cu_2O_5$ phases. If we recall the crystal structure of $YBa_2Cu_3O_{7-\delta}$, it is convincing that an electric-field gradient at ^{111}In(EC)^{111}Cd located at the Cu(1) site would not be strongly affected by the exchange of Y and Yb; but if it resides at the M site in $M_2Cu_2O_5$, the known different hyperfine interaction parameters[23] have to be found.

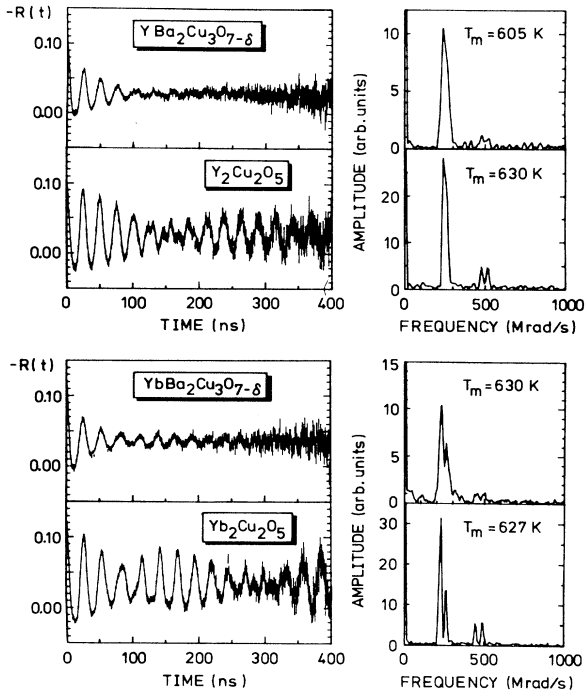

FIG. 2. Comparison of the $R(t)$ pattern (plus corresponding Fourier transforms) of ^{111}In(EC)^{111}Cd in $MBa_2Cu_3O_{7-\delta}$ with those of ^{111}In(EC)^{111}Cd in $M_2Cu_2O_5$, M=Y,Yb.

V. DISCUSSION

A. Impurity-phase model

The present experiments clearly show that for annealing temperatures $T_a \lesssim 1100$ K the hyperfine interactions found at ^{111}In(EC)^{111}Cd in $YBa_2Cu_3O_{7-\delta}$ (and in $YbBa_2Cu_3O_{7-\delta}$ as well) *do not* belong to regular sites of the superconducting $MBa_2Cu_3O_{7-\delta}$-structure but to the octahedrally coordinated M sites of the impurity phase $Y_2Cu_2O_5$ and $Yb_2Cu_2O_5$, respectively. Therefore, we have to withdraw our interpretation given in Refs. 34–36 and 65 where we attributed the hyperfine interactions $f_Y(1)$–$f_Y(3)$ to ^{111}In(EC)^{111}Cd substituting the Cu(1) site in $YBa_2Cu_3O_{7-\delta}$. Consequently, the observed hyperfine interactions during the orthorhombic–to–tetragonal phase transition[34] have to be attributed to the decompo-

TABLE II. Comparison of the hyperfine interaction parameters at ^{111}In(EC)^{111}Cd in $MBa_2Cu_3O_{7-\delta}$ with those found at ^{111}In(EC)^{111}Cd in $M_2Cu_2O_5$ (M=Y,Yb). To have a compatible set of data, the measurements were analyzed uniformly with three fractions (Ref. 23).

Compound	T_m [K]	(i)	f^i [%]	ν_Q^i [MHz]	η^i
$YBa_2Cu_3O_{7-\delta}$	605	$f_Y(1)$	30(2)	143(1)	1
		$f_Y(2)$	30(2)	159(1)	0.94(6)
		$f_Y(3)$	40(2)	193(10)	0.7(1)
$Y_2Cu_2O_5$	630	(1)	48(2)	144.3(5)	1
		(2)	48(2)	158.0(5)	0.95(1)
		(3)	4(4)	174(1)	0.84(2)
$YbBa_2Cu_3O_{7-\delta}$	630	$f_{Yb}(1)$	18(2)	138(1)	0.92(5)
		$f_{Yb}(2)$	18(2)	155(1)	0.84(2)
		$f_{Yb}(3)$	64(6)	163(5)	1
$Yb_2Cu_2O_5$	627	(1)	45(2)	136.3(5)	0.92(2)
		(2)	45(2)	152.7(3)	0.84(1)
		(3)	10(5)	175(1)	1

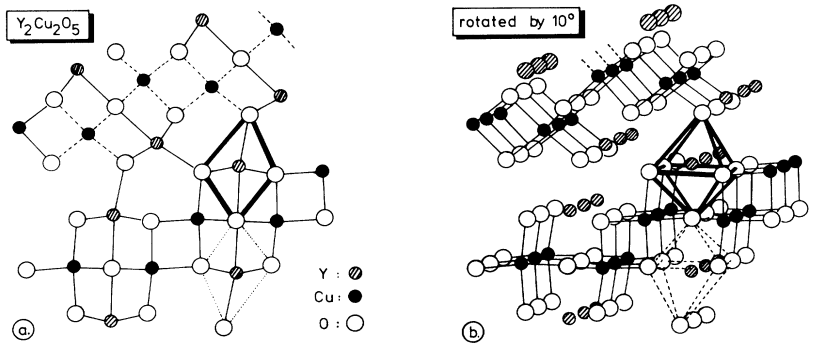

FIG. 3. (a) Structure of $Y_2Cu_2O_5$. A dotted line indicates the zig–zag line of fourfold oxygen coordinated Cu atoms. Also the position of two oxygen octahedra around the Y sites is indicated. (b) After rotation of the structure by 10° the position and shape of one octahedron is marked, the second one is indicated by dashed lines.

sition of $Y_2Cu_2O_5$ into $CuYO_2$.[60,61]

The most straightforward interpretation of these findings is the assumption of the existence of $Y_2Cu_2O_5$ precipitates, which incorporate all ^{111}In probes at moderate temperatures ($T_a \leq 1100$ K) but are too small to be detected by x-ray diffration.[34] At annealing and/or preparation temperatures of $T_a \approx 1100$ K these $Y_2Cu_2O_5$ precipitates decompose and nearly all ^{111}In probes substitute the Y site of $YBa_2Cu_3O_{7-\delta}$.[12,33,63] A further increase of the annealing temperature leads to the decomposition of $YBa_2Cu_3O_{7-\delta}$ into Y_2BaCuO_5. In this picture, only a small temperature window exists in which the element indium is soluble in $YBa_2Cu_3O_{7-\delta}$.

Besides the fact that such $Y_2Cu_2O_5$ precipitates have not been detected by conventional methods, there are some more *severe* objections to this *impurity phase assumption*: A clear channeling and blocking effect along the c axis of a c oriented thin $YBa_2Cu_3O_{7-\delta}$ film was observed after the implantation of ^{112m}In.[53] These data indicated that more than 40% of the ^{112m}In atoms occupy a regular site either in the –Cu(1)–O(4)–Cu(2)-row or in the –Y–Ba–Y row. Emission channeling only works if a continuous row leads the particle whereas a grain boundary would dechannel the particle. A similar argument holds for the observation of a distinct orientation dependence of the hyperfine interaction in a $YBa_2Cu_3O_{7-\delta}$ single crystal.[35] Finally, it is hard to understand why indium leaves an $Y_2Cu_2O_5$ precipitate in $YBa_2Cu_3O_{7-\delta}$ at ≈ 1100 K while it resides at the M site in $M_2Cu_2O_5$ up to 1275 K.[23]

B. Oxygen–defect model

As a solution of all these conflicting observations within the Cu(1)–site puzzle, we would like to propose a simple model that has the advantage of explaining all the observations mentioned but, unfortunately, cannot be proved directly. First we recall the facts known about the layered structure of $Y_2Cu_2O_5$ as given in Refs. 37, 71, and 72. Figure 3(a) shows the zig-zag line of fourfold coordinated Cu atoms. As described in Refs. 37 and 65 the oxygen atom which connects the two "Cu(1) sites" is below the plane of the other six oxygen atoms. The Y atoms of the "blue phase" sit each within an irregular oxygen octahedron between two layers of Cu–O chains. After a rotation of the lattice by 10° in Fig. 3(b), the typical arrangement of two octahedra between two short "Cu(1) chains" is visible.

Now we want to demonstrate that this typical structure element can be embedded in-between the $(CuO_2)_\infty$ planes of $YBa_2Cu_3O_{7-\delta}$. Figure 4(a) displays two unit cells of the $YBa_2Cu_3O_{7-\delta}$ structure. We assume that In^{3+} replaces an Y^{3+} just after its introduction. If two O(3) vacancies are created and the other two O(3) atoms are allowed to relax towards these vacancies, an oxygen octahedron [built by four O(2) and two O(3) atoms] around ^{111}In is found [see Fig. 4(b)]. In this way a basic unit of the $Y_2Cu_2O_5$ structure is obtained: irregular oxygen octahedra surround the Y site and also the next Cu atoms have a fourfold layered oxygen configuration comparable to that in $Y_2Cu_2O_5$. It agrees with a modern concept in crystallography that complicated structures like $YBa_2Cu_3O_{7-\delta}$ are composed of such substructures of their respective constituents.[73,74]

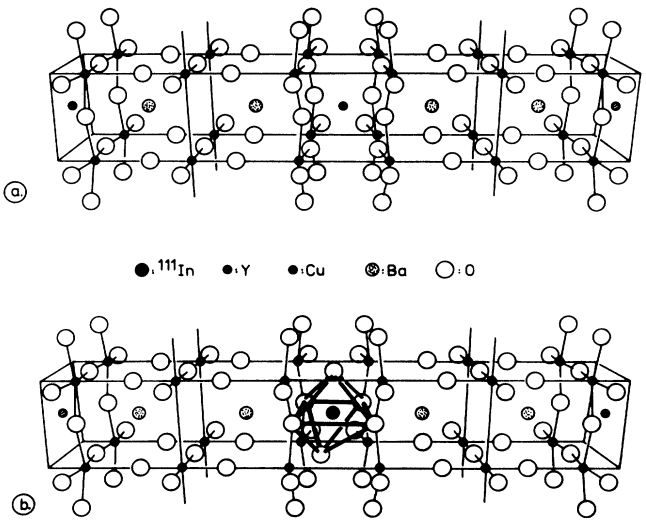

FIG. 4. (a) Two unit cells of $YBa_2Cu_3O_{7-\delta}$. (b) The proposed oxygen-defect complex with ^{111}In(EC)^{111}Cd at the Y site in $YBa_2Cu_3O_{7-\delta}$. Two O(2) oxygen atoms are removed and the other two are allowed to relax towards the vacancies. In this way the eightfold oxygen-coordination is changed to a sixfold one, leading to oxygen octahedra between the neighboring Cu–O chain like in $Y_2Cu_2O_5$.

The oxygen-defect model can now explain the observed channeling and blocking effect of positrons and electrons from ^{112m}In: in the direction of the c axis no change of the structure has appeared. As the oxygen–octahedron is oriented within the $YBa_2Cu_3O_{7-\delta}$ structure, the observed orientation dependence of the electric field gradient at ^{111}In(EC)^{111}Cd in the $YBa_2Cu_3O_{7-\delta}$ single crystal is also understood. Finally, at a temperature of $\approx$ 1100 K, this complex disappears when mobile oxygen atoms are trapped. The matrix rearranges itself to the correct $YBa_2Cu_3O_{7-\delta}$ structure and leaves ^{111}In on an unperturbed Y site.

VI. CONCLUSIONS

The oxygen–defect model explains all the hyperfine interactions found at ^{111}Cd in $MBa_2Cu_3O_{7-\delta}$ in most of the experiments. It solves the puzzle how to place the probe in an impurity phase and at the same time in the matrix. Unexpectedly, this model gives some insight in the process that forms the $YBa_2Cu_3O_{7-\delta}$ structure from its constituents; it also tells that in most cases $^{111}In^{3+}$ only substitutes Y^{3+}. As chemical parameters, like size and valency of the ion, determine the solubility and the site occupation of the probe in such a complex structure like $YBa_2Cu_3O_{7-\delta}$, further PAC experiments require the use of other probes, like, for example, ^{111}Ag$(\beta^-)^{111}$Cd, which seems to promise local information from the $(CuO_2)_\infty$ planes and/or $(CuO)_\infty$ chains of $YBa_2Cu_3O_{7-\delta}$.[53]

ACKNOWLEDGMENTS

We would like to thank H. Thomas for the skillful preparation of so many samples of equally good quality, our colleagues of the Göttingen HTSC collaboration and K. P. Lieb for their continuous support. We also thank H. Plank, R. Polewka, W. Witthuhn, and L. Hamdi for many fruitful and cheerful discussions. This work was supported by the BMFT under Contract No. 13N5493.

[1] J.G. Bednorz and K.A. Müller, Z. Phys. B **64**, 189 (1986).
[2] C.W. Chu, P.H. Hor, R.L. Meng, L. Gao, Z.J. Huang, and Y.Q. Wang, Phys. Rev. Lett. **58**, 405 (1987).
[3] M.K. Wu, J.R. Ashburn, C.J. Torng, P.H. Hor, R.L. Meng, L. Gao, Z.J. Huang, and C.W. Chu, Phys. Rev. Lett. **58**, 908 (1987).
[4] P. Bordet, J.J. Capponi, J.L. Hodeau, M. Marezio, R.J. Cava, A.W. Hewat, E.A. Hewat, and A. Santoro, Eur. J. Solid State Inorg. Chem. **27**, 57 (1990).
[5] F. Pleiter and C. Hohenemser, Phys. Rev. B **25**, 106 (1982).
[6] G.S. Collins, S.L. Shropshire, and J. Fan, Hyperfine Interact. **62**, 1 (1990).
[7] G.S. Collins and J. Fan, Hyperfine Interact. (to be published).
[8] T. Wichert, W. Witthuhn, H. Metzner, and R. Sielemann, in *Hyperfine Interactions of Defects in Semiconductors*, edited by G. Langouche (Elsevier, Amsterdam, 1992), Chap. 2, p. 79.
[9] M. Deicher, Nucl. Instrum Methods B **63**, 189 (1992).
[10] H. Skudlik, M. Deicher, R. Keller, R. Magerle, W. Pfeiffer, D. Steiner, E. Recknagel, and Th. Wichert, Phys. Rev. B **46**, 2159 (1992).
[11] N. Achtziger and W. Witthuhn, Phys. Rev. B **47**, 6990 (1993).
[12] J.A. Gardener, R. Wang, R. Schwenker, W.E. Evenson, R. Rasera, and J. Sommers, in *Proceedings of the XXV Zakopane School on Physics*, edited by J. Stanek (World Scientific, Singapore, 1991), p. 25.
[13] R. Wang, J.A. Gardener, W.E. Evenson, and J. Sommers, Phys. Rev. B **47**, 638 (1993).
[14] D. Wiarda, M. Uhrmacher, A. Bartos, and K.P. Lieb, J. Phys.: Condens. Matter **5**, 4111 (1993).
[15] W. Bolse, A. Bartos, J. Kesten, K.P. Lieb, and M. Uhrmacher, Ber. Bunsen-Ges. Phys. Chem. **93**, 1285 (1989).
[16] G. Krausch, T. Detzel, R. Fink, B. Lukscheiter, R. Platzer, U. Wöhrmann, and G. Schatz, Phys. Rev. Lett. **68**, 377 (1992).
[17] A. Bartos, W. Bolse, K.P. Lieb, and M. Uhrmacher, Phys. Lett. A **131**, 471 (1988).
[18] M. Uhrmacher, A. Bartos, and W. Bolse, Mat. Sci. Eng. A **116**, 129 (1989).
[19] K.P. Lieb, T. Weber, M. Uhrmacher, Z. Inglot, and A. Bartos, in *Proceedings of XXVI Zakopane School on Physics*, edited by J. Stanek (World Scientific, Singapore, 1992), p. 118.
[20] W. Bolse, M. Uhrmacher, and K.P. Lieb, Phys. Rev. B **36**, 1818 (1987).
[21] A. Bartos, K.P. Lieb, A.F. Pasquevich, M. Uhrmacher, and ISOLDE Collaboration, Phys. Lett. A **157**, 513 (1991).
[22] J. Shitu, D. Wiarda, T. Wenzel, M. Uhrmacher, K.P. Lieb, S. Bedi, and A. Bartos, Phys. Rev. B **46**, 7987 (1992).
[23] A. Bartos, M. Uhrmacher, and K.P. Lieb, J. Alloys and Compounds **179**, 307 (1992).
[24] G.L. Catchen, S.J. Wukitch, E.M. Saylor, W. Huebner, and M.A. Blaszkiewicz, Ferroelectrics **117**, 175 (1991).
[25] T.M. Rearick, G.L. Catchen, and J.M. Adams, Phys. Rev. B **48**, 224 (1993).
[26] D. Wiarda, T. Wenzel, M. Uhrmacher, and K.P. Lieb, J. Phys. Chem. Solids **53**, 1199 (1992).
[27] A. Bartos, D. Wiarda, Z. Inglot, K.P. Lieb, M. Uhrmacher, and T. Wenzel, J. Phys.: Condens. Matter (to be published).
[28] A. Bartos, K.P. Lieb, M. Uhrmacher, and D. Wiarda, Acta Cryst. B **49**, 165 (1993).
[29] D. Lupascu, A. Bartos, K.P. Lieb, and M. Uhrmacher (unpublished).
[30] J.A. Gardener, H.T. Su, A.G. McKale, S.S. Kao, L.L. Peng, W.H. Warnes, J.A. Sommers, K. Athreya, H. Franzen, and S.-J. Kim, Phys. Rev. B **38**, 11317 (1988).
[31] P. Singh, M.N. Nyayate, S.H. Devare, and H.G. Devare, Hyperfine Interact. **50**, 516 (1989).
[32] P. Singh, M.N. Nyayate, S.H. Devare, and H.G. Devare, Phys. Rev. B **39**, 2308 (1989).
[33] H. Plank, O. Bauer, D. Forkel, F. Meyer, B. Roas, G. Saemann-Ischenko, J. Ströbel, H. Wolf, and W. Witthuhn, Hyperfine Interact. **61**, 1139 (1990).
[34] A. Bartos, M. Uhrmacher, and H.U. Krebs, Phys. Lett. A **142**, 181 (1989).

[35]M. Uhrmacher, A. Bartos, and K. Winzer, J. Less-Common Metals **150**, 185 (1989).
[36]M. Uhrmacher and A. Bartos, in *Proceedings of XXIV Zakopane School on Physics*, edited by J. Stanek (World Scientific, Singapore, 1990), p. 25.
[37]A. Bartos and M. Uhrmacher, Hyperfine Interact **61**, 1101 (1990).
[38]J.M. Tarascon, W.R. McKinnon, L.H. Greene, G.W. Hull, and E.M. Vogel, Phys. Rev. B **36**, 226 (1987).
[39]T.J. Kistenmacher, J. Appl. Phys. **64**, 5067 (1988).
[40]G. Schatz and A. Weidinger, *Nukleare Festkörperphysik* (Teubner, Stuttgart, Germany, 1985).
[41]*Hyperfine Interaction of Radioactive Nuclei*, edited by J. Christiansen (Springer, Berlin, Germany, 1983).
[42]H.H. Rinneberg, Atomic Energy Review **17**, 477 (1979).
[43]H. Frauenfelder and R. Steffen, in *Alpha–, Beta–, Gamma–Ray Spectroscopy*, edited by K. Siegbahn (North-Holland, Amsterdam, Netherlands, 1965).
[44]M. Yates, in *Alpha–, Beta–, Gamma–ray Spectroscopy* (Ref. 43).
[45]F. James and M. Roos, Program MINUIT, CERN Computer Center, program library D506/516 (1977).
[46]J.D. Roger and A. Vasquez, Nucl. Instrum. Methods **130**, 539 (1975).
[47]J. Chunlin, C. Chuanmeng, W. Kuihan, L. Sulan, Z. Guiyi, Z. Guofan, Q. Cuenfu, B. Weiming, F. Zhanguo, and X. Qian, Solid State Commun. **65**, 859 (1988).
[48]D.H.A. Blank, H. Kruidhof, and J. Flokstra, J. Phys. D **21**, 226 (1988).
[49]M. Uhrmacher, K. Pampus, F. J. Bergmeister, D. Purschke, and K.P. Lieb, Nucl. Instrum. Methods B **9**, 234 (1985).
[50]J. Ziegler and J. Biersack, *The Stopping and Range of Ions in Solids* (Pergamon, New York, 1985).
[51]O. Meyer, J. Geerk, T. Kröner, Q. Li, G. Linker, B. Strehlau, and X. Xi, Mater. Res. Soc. Symp. Proc. **157**, 493 (1990).
[52]T. Kröner (unpublished).
[53]A. Bartos, H. Plank, D. Forkel, S. Jahn, J. Markel, R. Polewka, M. Uhrmacher, S. Winter, W. Witthuhn, and ISOLDE Collaboration, J. Less Common Metals **164&165**, 1121 (1990).
[54]H. Lütgemeier, Hyperfine Interact. **61**, 1051 (1990).
[55]I. Felner, Thermochimica Acta **174**, 41 (1991).
[56]T.J. Kistenmacher, Phys. Rev. B **38**, 8862 (1988).
[57]T. Siegrist, L.F. Schneemeyer, J.V. Waszczak, N.P. Singh, R.L. Opila, B. Batlogg, L.W. Rupp, and D.W. Murphy, Phys. Rev. B **36**, 8365 (1987).
[58]R. Bormann and J. Nölting, Appl. Phys. Lett. **54**, 2148 (1989).
[59]H.U. Krebs, J. Less-Common Metals **150**, 269 (1989).
[60]A. Bartos, Ph.D. thesis, University of Göttingen, Germany, 1991.
[61]H. Saitovich, P.R.J. Silva, and A.M. Rodriguez, Hyperfine Interact. **73**, 277 (1992).
[62]H. Plank, F. Meyer, and W. Witthuhn, Phys. Lett. A **133**, 451 (1988).
[63]H. Plank, Ph.D. thesis, University of Erlangen, Germany, 1991.
[64]R. Polewka, diploma thesis, University of Erlangen, Germany, 1990.
[65]M. Uhrmacher and A. Bartos, Hyperfine Interact. **61**, 1073 (1990).
[66]C. Michel and B. Raveau, J. Solid State Chem. **43**, 73 (1982).
[67]R.M. Hazen, L.W. Finger, R.J. Angel, C.T. Prewitt, N.L. Ross, H.K. Mao, C.G. Hadidiacos, P.H. Hor, R.L. Meng, and C.W. Chu, Phys. Rev. B **35**, 7238 (1987).
[68]H. Scheel and F. Licci, Thermochimica Acta **174**, 115 (1991).
[69]R. Jones, R. Janes, R. Armstrong, N.C. Pyper, P.P. Edwards, D.J. Keeble, and M.R. Harrison, J. Chem. Soc. Faraday Trans. **86**, 675 (1990).
[70]M. Uhrmacher and A. Bartos, Hyperfine Interact. **61**, 1113 (1990).
[71]J. Aride, S. Flandrois, M. Taibi, A. Boukhari, M. Drillon, and J.L. Soubeyroux, Solid State Commun. **72**, 459 (1989).
[72]C. Müller, diploma thesis, University of Kiel, Germany, 1989.
[73]G. Pathe (private communication).
[74]P. Fagan and M. Ward, Sci. Am. July, 28 (1992).
[75]G.L. Catchen, M.A. Blaszkiewicz, A.J. Baratta, and W. Huebner, Phys. Rev. B **38**, 2824 (1988).
[76]M. Blaszkiewicz, Ph.D. thesis, The Pennsylvania State University, Pennsylvania, 1989.